

Synthesis of nano powder composite of tantalum carbide-boride

BEHZAD MEHDIKHANI*, GHOLAM HOSSEIN BORHANI

Department of Materials Engineering, Malek-e-ashtar University of Technology, Isfahan, Iran

In this study, mechanochemical process (MCP) is applied to synthesize ultrafine TaC powders. In this research, submicron composite powder TaC-TaB₂ was produced using mixtures of tantalum carbide and boron carbide as raw materials via mechanochemical process. The phase formation characterization during process was utilized by X-ray diffractometry (XRD). The morphology of synthesized powder was studied using scanning electron microscopy (SEM).

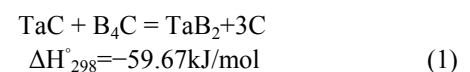
(Received July 31, 2013; accepted May 15, 2014)

Keywords: Mechanochemical process (MCP), Tantalum carbide, TaC-TaB₂ Composite

1. Introduction

Development of the ceramic matrix composites (CMCs) that combine advantageous properties of the individual components for high performance applications is of special interest to the ceramic industry [1]. For example, the composites of boride and carbide offer an attractive combination of excellent mechanical and electrical properties, which renders them promising candidates for the advanced structural applications at high temperatures and/or in corrosive environments. With the rapid development of aerospace technology, it is urgent to study the new material used in high temperature structural components [2]. Tantalum Carbide (TaC) is an ultra high-temperature ceramic (UHTCs) for high performance applications with a melting point in excess of 3900°C [1-3]. Unique combination of good chemical stability, good corrosion resistance, high modulus (537GPa), high hardness (15–19GPa) and other good mechanical properties make it a candidate material for rocket propulsion components [4-5] and many applications as high speed cutting tools, wear resistant parts, hard coating on hard metals and high temperature structural materials [1]. Performance of this material at high temperature needs good oxidation resistance [5]. Researchers have been found that TaB₂ is suitable additives [4]. Tantalum borides have not been studied as extensively as other borides, like TiB₂ [6], ZrB₂ [7], and HfB₂ [8]. According to the Ta–B phase diagram [9], there are five boride phases including Ta₂B, Ta₃B₂, TaB, Ta₃B₄, and TaB₂. Besides, a new phase Ta₅B₆ and its crystal structure were later identified by Bolmgren et al. [10]. On the formation of tantalum borides, a variety of processing routes have been utilized.

For example, Hideaki et al. [11] produced TaB₂, TaB, and Ta₃B₄ by solid state reactions of mixed Ta and amorphous boron powders under corresponding compositions at 800, 900, and 1800°C, respectively. Peshev [12] obtained TaB₂ through borothermic reduction of Ta₂O₅ at 1650°C for 1 h. Tantalum diboride (TaB₂) with comparable mechanical properties to ZrB₂ and HfB₂ was also fabricated by reducing Ta₂O₅ with B₄C and graphite at 1600°C. The ternary phase diagram is known since the 1963 in Fig. 1 [13]. It is well known that the properties of composite TaC-TaB₂ are strongly dependent on the relative amounts and types of the various phases formed. It has to be noted that B₄C, which is also a component of the Ta–C–B ternary system, is not chemically compatible with Ta or TaC. It reacts with Ta and TaC forming TaB₂ and free Carbon that has been used for the synthesis and processing of diboride-containing ceramics [14]. Recently, mechanical activation and mechanical milling have been extensively used for synthesis of advanced materials. The technological advantages of the mechanochemical synthesis are obvious. High-temperature processes and furnaces for synthesis of this composite are avoided. The product obtained is finely dispersed and has a defect structure which increases the sinterability of TaC-TaB₂ powder. This article demonstrates the formation of TaC-TaB₂ by ball milling a mixture of TaC and B₄C with the stoichiometry of reaction (1):



The negative value of ΔH_{298}° suggests that this reaction is exothermic and should be self-sustaining.

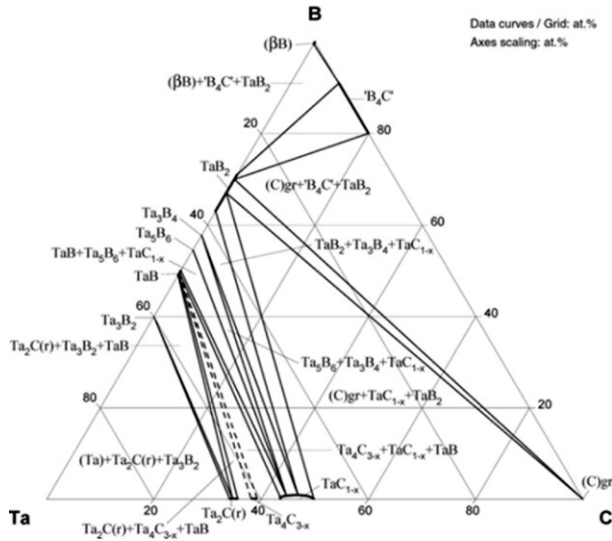


Fig. 1. Ternary diagram B-Ta-C [14].

2. Experimental

2.1- Raw material

The starting powders were TaC(Ningxia Orient Tantalum Industry Co., Ltd., China), and B₄C (Jingangzuan Boron Carbide Co. Ltd., China) with mean particle size 1.25 μm and 300 nm, respectively. The TaC content in the TaC powder was higher than 99%. The main impurities were ~0.3 wt% Nb, 0.1 wt% Fe, 0.20 wt% O, 0.15 wt% free carbon, 0.05 wt% N, and Al, Ca, K, Na, Ti with a total amount <0.05 wt%. The B₄C was >95 wt% pure with major impurities of free carbon.

2.2. Powder preparation

25g TaC and 2.0%Wt. B₄C were mixed in a WC cylinder(250ml) using 150gr WC balls as mixing media. Ball milling of powder mixture was carried out in a planetary ball mill at room temperature in n-hexane and under argon atmosphere. The ball-to-powder weight ratio and the rotational speed of vial were 20:1 and 250 rpm, respectively for 3, 6 and 12 hours. The milling was interrupted at selected times and a small amount of powder was removed for further characterizations.

2.3. XRD analysis

Phase transformation during milling were determined by X-ray diffraction (XRD) in a Philips X'PERT MPD diffractometer using filtered Co K α radiation ($\lambda = 0.178$ nm). The lattice parameter of a cubic substance is directly proportional to the spacing 'd' of any particular set of lattice planes (Eq:2) [15].

$$a = \frac{d}{\sqrt{h^2 + i^2 + j^2}} \quad (2)$$

the Nelson–Riley method was used to minimize errors caused by aberration of 2θ variation and the lattice parameter 'a' of TaC was calculated for at least three peaks, using Eq. (3) [16].

$$F(\theta) = \frac{1}{2} \left(\frac{\cos^2 \theta}{\sin \theta} + \frac{\cos^2 \theta}{\theta} \right) \quad (3)$$

Silicon standard sample with large grains and free from defect broadening was used as a standard to increase the precision of the instrumental broadening. Then, the error of diffractometer was eliminated by Eq. (4) [27].

$$b = \gamma_{size} + \gamma_{strain} = \sqrt{b_0^2 - \gamma_s^2} \quad (4)$$

Where 'b_s' is the FWHM of the main peak of Si standard sample ($2\theta=28.5^\circ$) used for calibration and 'b₀' is the FWHM of TaC's peaks. Both 'b_s' and 'b₀' were calculated by X-Pert High Score software. Crystallite size and internal strain of specimens were calculated from broadening of XRD peaks using the Williamson-Hall method [17].

$$\beta \cos \theta = K\lambda / d + \mu \sin \theta \quad (5)$$

Where θ is the Bragg diffraction angle, d is the average crystallite size, k is a constant (with a value of 0.9), λ is the wavelength of the radiation used, and β is the diffraction peak width at half maximum intensity.

The morphology and microstructure of milled powder particles were examined by SEM images in a Philips XL30 at an accelerating voltage of 30 kV.

2.4. Morphology of powders

The morphology of selected mechanically alloyed powders was examined by a Scanning Electron Microscope (SEM-Philips XL30) operating at 30 kV.

3. Result and discussion

3.1. X-Ray diffraction

A commercial software program (HSC Chemistry) was used to identify the probable reaction using thermodynamic data. Fig. 2 shows X-ray diffraction patterns of the TaC and TaC-TaB₂ powder after various milling time. Fig. 2-a shows XRD pattern of raw tantalum carbide powder without milling. Fig. 2-b shows XRD pattern of powder after 3 hours milling were identified as a mixture of starting materials. The results show that the powder milled for 3 hours, no new phase is not formed. B₄C phase in the XRD spectra have been observed in some detail because it is a small amount of 2% wt. Fig. 2-c shows the XRD results of the powders milled for 6 hours, TaB₂ phase unformed and there are still some B₄C composition. The XRD analysis indicated that only TaB

and TaB₂, as presented in Fig. 2-d, were produced from the samples of their equivalent stoichiometries. Fig. 2-d shows that the final products obtained from mechanochemical synthesis was free from three Ta-rich samples of Ta₂B= 2:1,

Ta₃B₂=3:2 and Ta₃B₄=3:4 contain a large amount of residual Ta. No XRD peaks were observed for B₄C, suggesting that a reaction had occurred in the system. Cup and balls of ball mill was made from WC so X-ray results show that increasing milling time up to 12 hours has caused a spike tungsten carbide Fig. 2-d.

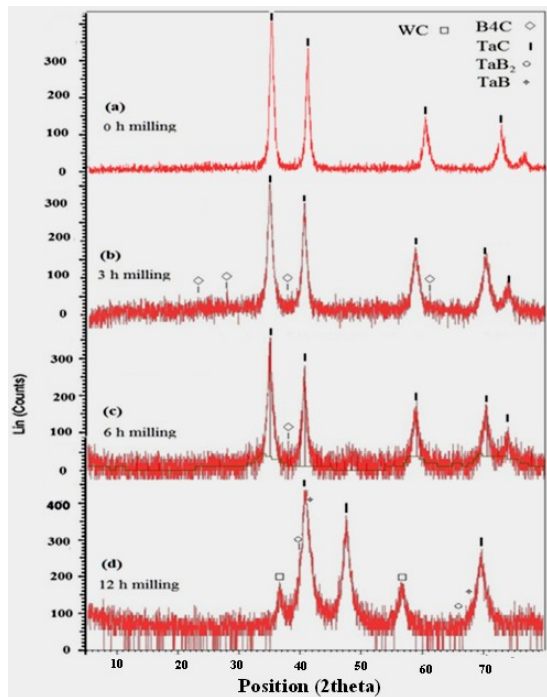


Fig. 2. XRD patterns of TaC-B₄C powder after various milling time: (a) 0, (b) 3, (c) 6, and (d) 12 h.

The lattice parameter of TaC powder obtained from 3, 6 and 12 h milling is calculated by Nelson–Riley method from the XRD analysis (Fig.3). In this method, the accurate lattice parameter is obtained by extending the lattice parameter function and its connection to zero content of Nelson–Riley parameter. Fig. 3 shows that the lattice parameter increases by increasing milling time. The change of lattice parameter of milled samples for 3, 6 and 12 h is presented in Table 1.

Table 1. The lattice parameter of TaC powder after 3, 6 and 12 h milling times.

Milling time, h	Lattice parameter, Å Nelson–Riley method
3	4.3242
6	4.4063
12	4.4526

From Table 1, it is concluded that there is little decrease in the lattice parameter by increasing milling time. The grain size 'd' and strain 'μ' of TaC products during milling were measured by the Williamson–Hall method (Fig. 4). The FWHM of the diffraction peak is wider with milling time due to the strain and the refinement of powder. A plot of B cosθ versus sinθ [18] is shown in Fig. 4. The average grain sizes of the TaC calculated from the XRD data were about 801, 267, 94 and 34 nm for the samples with milling times of 0, 3, 6, and 12 h. According Eq.(5) and Williamson-Hall method calculation, internal strain and crystallite size of milled powder is shown in Fig. 5. Internal strain of powders has increased with increasing milling time and crystallite size is reduced.

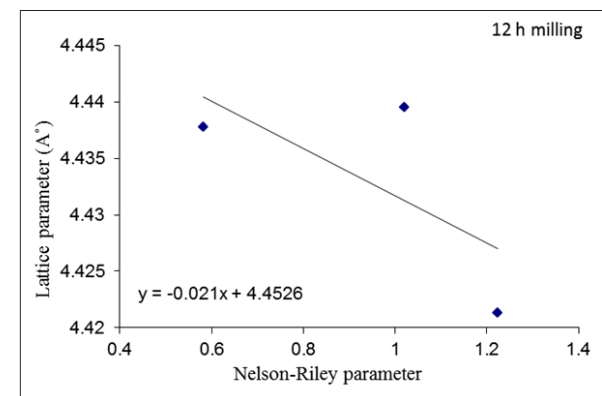
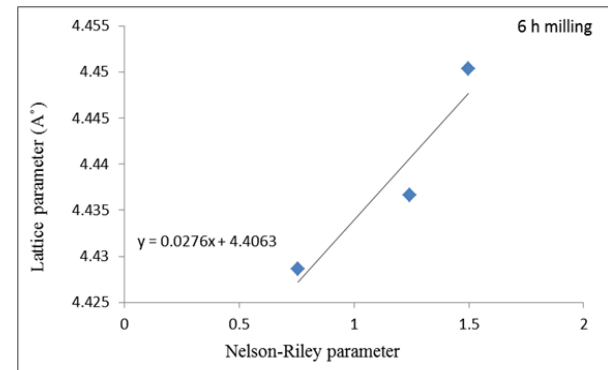
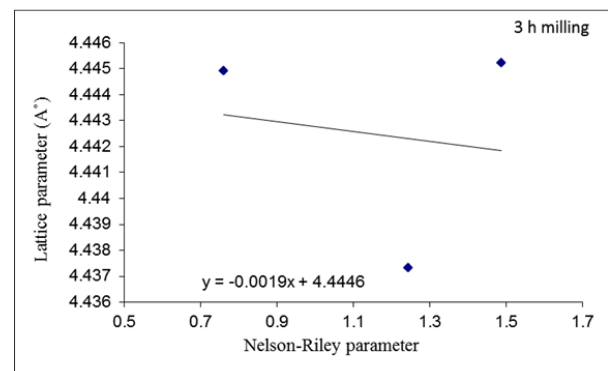


Fig. 3. Nelson–Riley parameter for obtaining the lattice parameter of TaC phase after 3, 6 and 12 milling times.

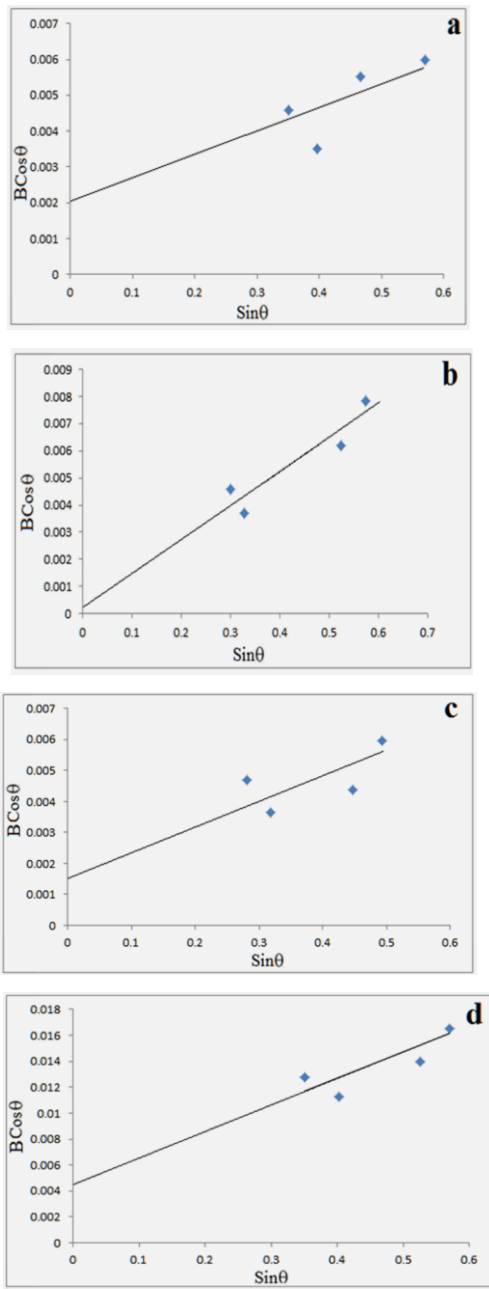


Fig. 4. Plot of $B\cos\theta$ versus $\sin\theta$ for TaC- B_4C milled powders: (a) 0, (b) 3, (c) 6, and (d) 12 h.

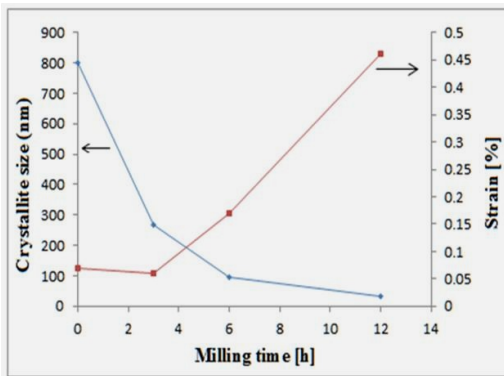


Fig. 5. Effect of milling time on the crystallite size and internal strain of powders.

3.2. Microscopic examinations

SEM images of TaC powder with milling time are shown in Fig. 6. This figure shows morphology of powder particles after different milling times. SEM images of TaC powder with milling time are shown in Fig. 6. The TaC powder without milling has an angular shape. Fig. 6-b shows that particle size reduction after 3 h of milling. At the beginning of the milling process, the brittle particles (TaC) got fragmented and comminuted and TaC powder gets rounder shape and comes refinement with milling time. After 6 h Fig. 6-c, the powder particles became nearly equiaxed in shape with a wide size distribution of 0.3-1 μm . By increasing milling time to 12 h the rate of fracturing increased and as a result the size of powder particles decreased. At this stage, the morphology of powder particles was almost equiaxed Fig. 6-d. The powder particles after 12 h of milling time are large agglomerates of ultrafine particles ranging from 0.1 μm to 2 μm .

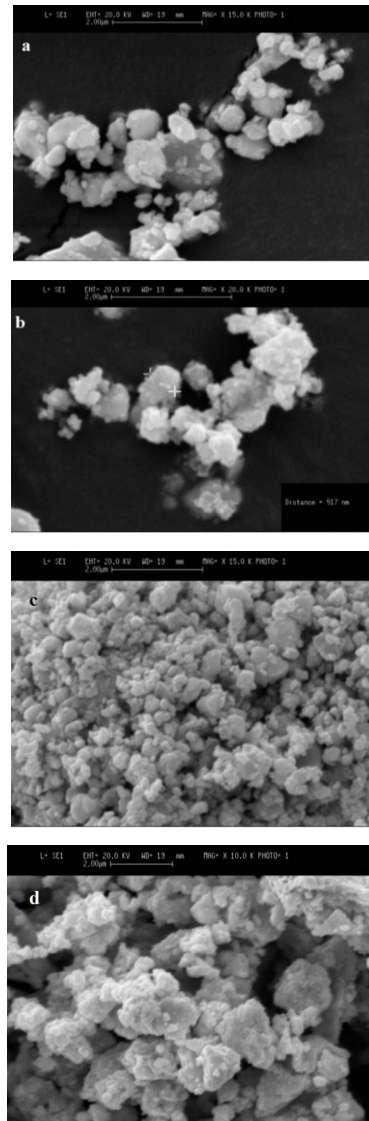


Fig. 6. SEM micrographs of starting powders particles (a) TaC powder, (b) after 3 h, (c) after 6 h and after (d) 12 h of milling times.

4. Conclusion

TaC-TaB₂ composite powder has been synthesised by a low temperature solid-state reaction between tantalum carbide and boron carbide. Studies show that by milling of powders TaC and B₄C, TaB₂ phase and the resulting composite TaC-TaB₂ is composed. Prolonging the milling time up to 12 h resulted in a decrease of grain size to nanoscale along with increasing strain and a slight increase in lattice parameter of TaC phase. Crystallite size of milled powder decreased with increasing milling time up to 3, 6 and 12 h. the powder particle size reached to 267 were 94 and 34 nm. TaB₂ phase in the powder milled for 12 h was observed, indicating that some mechanochemical synthesis process is carried out. Increasing milling time was increased internal strain of crystallites.

Acknowledgement

The authors are indebted to material department in Malek-e-ashtar University of Technology, that supplied the raw materials for the development of this research and to building and construction department of Standard Research Institute for its equipment support.

References

- [1] T. H. Squire, J. Marschall, J. European Ceramic Society. **30**, 2239 (2010).
- [2] F. Monteverde, A. Bellosi, L. Scatteia, J. Materials Science and Engineering. **485**, 415 (2008).
- [3] D. Hwan Kwon, S. H. Hong, B. K. Kim, J. Materials Letters. **58**, 3863 (2004).
- [4] X. Zhang, G. E. Hilmas, W. G. Fahrenholtz, J. Materials Science and Engineering. **501**, 37 (2009).
- [5] G. Hagemann, H. Immich, T. V. Nguyen, E. Gennady, Advanced Rocket Nozzles, J. Propulsion and powder. 14 (1998).
- [6] R. G. Munro, J. Res. Natl. Inst. Stand. Technol. **105**, 709 (2000).
- [7] W. G. Fahrenholtz, G. E. Hilmas, I. G. Talmy, J. A. Zaykoski, J. Am. Ceram. Soc. **90**, 1347 (2007).
- [8] R. Licheri, R. Orru, C. Musa, A. M. Locci, G. Cao, J. Alloys Compd. **478**, 572 (2010).
- [9] T. B. Massalski, H. Okamoto, P. R. Subramanian, L. International Materials Park, OH, USA, 1996.
- [10] H. Bolmgren, T. Lundström, L. E. Tergenius, S. Okada, I. Higashi, J. Less Comm. Met. **161**, 341 (1990).
- [11] I. Hideaki, S. Yusuke, K. Satoshi, N. Shigeharu, J. Ceram. Soc. Jpn. **98**, 264 (1990).
- [12] P. Peshev, L. Leyarovska, G. Bliznakov, J. Less Comm. Met. **15**, 259 (1968).
- [13] P. Rogl, Boron – Carbon – Tantalum, Springer 2009.
- [14] I. G. Talmy, J. A. Zaykoski, M. M. Opeka, J. European Ceramic Society, **30**, 2253 (2010).
- [15] B. D. Cullity, Elements of X-ray Diffraction, 2nd ed. Addison-Wesley, Inc., Massachusetts, 1956.
- [16] J. B. Nelson, D. P. Riley, Proceedings of the Physical Society **57**, 160 (1945).
- [17] G. K. Williamson, W. Hall, J. Acta Metall. **1**, 22 (1953).
- [18] C. Suryanarayana, M. Grant Norton, Plenum Press, New York, 1998.

*Corresponding author: beh_mehdikhani@yahoo.com